

# Validation of power output modelling of an agrivoltaic system with on-site measurements in Palaiseau, France

Moira I. TORRES AGUILAR<sup>1</sup>, Shusen YU<sup>2</sup>, Anne MIGAN-DUBOIS<sup>1,3</sup>, Jordi BADOSA FRANCH<sup>2</sup>, Bouchra MEKHALDI<sup>2</sup>, Johan PARRA<sup>2</sup>, Vincent BOURDIN<sup>1,3,4</sup>

<sup>1</sup> Université Paris-Saclay, CentraleSupélec, CNRS, Laboratoire de Génie Électrique et Électronique de Paris, 91192 Gif-sur-Yvette, France

<sup>2</sup> LMD/IPSL, Ecole Polytechnique, IP Paris, Sorbonne Université, ENS, PSL University, CNRS – 91128 – France

<sup>3</sup> Sorbonne Université, CNRS, Laboratoire de Génie Électrique et Électronique de Paris, 75252 Paris, France

<sup>4</sup> CNRS, LISN, Bâtiment 507, Rue du Belvédère, 91405 Orsay, France

**RESUME** – The need to address growing water, food, and renewable energies challenges has led to agrivoltaics, a photovoltaic (PV) application, to continue to gain importance since it increases food production while reducing water usage for farming and generates energy. Bifacial modules are uniquely positioned to contribute to the development of agrivoltaics, making it necessary to do extensive analysis of their on-site performance at different locations. Modelling makes it possible to analyze the impact of PV modules on the development of various crops and vice versa, bridging the gap between theory and practice. This work presents the results of modelling the operation of a bifacial module in an agrivoltaics installation located in Palaiseau, France. From the ideal tilt angle to reduce self-shading using backtracking, to its power output. Our findings show that while existing irradiance, temperature, and power models provide adequate estimations for a horizontal position, there is a variation in error when in backtracking mode. For the front irradiance there is an increase in relative mean bias error of 4.2%, from 3.64% to 7.84%. For the back irradiance the underestimation increases by 2.82%, from -5.28% to -8.10%. This change for the backface irradiance is impacted by an increase in albedo of 4% due to the presence of crops. The mean bias error for the module temperature was 0.94 °C in a horizontal position and 0.64 °C in backtracking. For the power output, an effective irradiance calculated with modelled irradiances led to an overestimation of 11.82% when in a horizontal position compared to 16.08% in backtracking. For irradiance yield, the presence of crops during the months of July and August contributes to an increased yield from the backface of the module. In terms of shading, the lack of neighboring modules in the southern extremity of the string will result in a yield up to 4.6% higher than those located in the center. Due to shadows caused by the meteorological station located between PV rows, there is a loss of yield of up to 17.43% between central modules and those located on the northern extremity of the string. In terms of performance, there is an increase in performance ratio with respect to a monofacial module of 9% during summer and of 11% during winter.

## Key-words:

*Agrivoltaics, tracking, backtracking, PV modelling, bifaci*

## 1. INTRODUCTION

According to the Mediterranean IPCC [1], the Euro-Mediterranean area is one key region where action is needed to address water, food, and energy demand. For this reason, agrivoltaics is a PV application that has gained importance since

it increases food production while reducing water usage for farming combined with energy generation. Studies such as [2] show the best environment for crops to grow is simultaneously ideal for PV power generation, in [3] their results indicate that the combined land use is more productive than using the land solely for crops.

Supported by advances such as bifacial modules, and government-led initiatives worldwide, the global agrivoltaics market size is estimated at USD 5.13 billion in 2025 and is predicted to reach around USD 13.88 billion by 2034. In 2024 Europe had a market share of 29%, behind only North America with a share of 33% [4].

Bifacial modules are uniquely equipped to improve the energy generation of an agrivoltaic installation due to their ability to generate electricity from both sides. Their performance characterization and modelling however is complex due to the variety of factors that can influence their energy production as explained in [5].

For this reason, accurate irradiance modelling is essential to the study of agrivoltaics since the contributions from both front and back need to be considered for estimating the power output of an installation.

Additional research regarding the power output of an installation at different locations is needed since studies such as [6] have shown that depending on the location certain system designs may be better suited than others and the difference in energy yield between single-axis or dual-axis tracking may be of only 2% .

The present work is focused on the preliminary results of a step-by-step modelling chain starting with the tilt angle of a module in backtracking mode, followed by the front and back irradiance, module temperature, and finally the DC power output of a single module in an agrivoltaics farm installed in 2024 at the SIRTA research observatory [7] in Palaiseau, France. Modelling errors are presented for the two periods of module position: horizontal and backtracking. Additionally, the influence on the modelling errors for front and back irradiance of albedo change due to crop growth is briefly addressed.

A general performance characterization with indicators such as reference yield, module yield, and performance ratio is also

presented. The impact on back irradiance of an increased albedo due to the presence of plants is shown. Other factors impacting performance such as soiling and shading are also mentioned.

## 2. DEMONSTRATOR

The installation, shown in Fig. 1, consists of 72 half-cell c-Si TOPCon based photovoltaic panels with a nominal power between 555-565 W and a bifaciality factor of 0.80. They have a North-South orientation with 1 axis of tracking (East-West) and are divided into 4 strings, consisting each of 18 panels connected in series, with each string connected to an inverter. In addition, modules of the second and third row are equipped with optimizers and are divided into 4 groups (A, B, C, D) and numbered 1 through 9. The disposition of the modules is shown below.

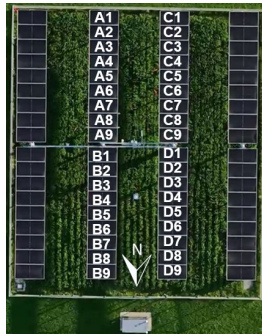


Figure 1 AgriPV installation located on the campus of Ecole Polytechnique in Palaiseau, France. Letter and number identifying each individual module is shown..

The module studied in the present work, shown in Fig. 2 as A8 and hereafter referred to as “test module”, is equipped with 4 irradiance c-Si reference cells: 2 upward and 2 downward facing located on each corner. It is also fitted with 2 temperature probes: one on each half of the module but close to the center.

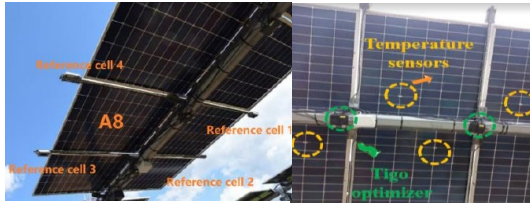


Figure 2 Location of irradiance reference cells in test module (left), of optimizer and temperature probes (right).

In addition, a meteorological station measuring environmental variables such as air temperature, precipitation, horizontal irradiance is located between modules A9, C9, B1, and D1. Some soil measurements such as a moisture profile at different depths, ground temperature, and ground humidity are also available.

The period analyzed in this work is from June 2024 to March 2025. During this time there were two distinct intervals: June 1<sup>st</sup> – November 19<sup>th</sup> 2024 where all modules were kept in a horizontal position and November 20<sup>th</sup> 2024 – March 31<sup>st</sup> 2025 where the modules were set to backtracking mode in order to minimize the shading between the modules throughout the day.

Furthermore, there were two periods of alfalfa crop growth and recollection: February 7<sup>th</sup> – August 29<sup>th</sup> 2024 and August 30<sup>th</sup> – November 19<sup>th</sup> 2024. A third period of alfalfa growth started on February 20<sup>th</sup> 2025.

## 3. PV MODELLING

### 3.1. Tilt angle

The first step was to model the optimal tilt angle between rows to minimize self-shading at every moment of the day using the open-source python toolbox “PVlib”. The best fit with the measured single-axis tracker angles was found by varying the ground coverage ratio (GCR), ratio of the photovoltaic array to total ground area, which was calculated using the row pitch given by the installation company and module measurements provided by the manufacturer.

In Fig. 3, a variation of GCR between 0.42 and 0.47 is shown. A value of 0.44 leads to a mean bias error (MBE) of 0.35° and a mean absolute error (MAE) of 1.75°, resulting in the best agreement with the measured angles. This GCR value is applicable to all rows since the difference in tracker angle between them is less than 1°.

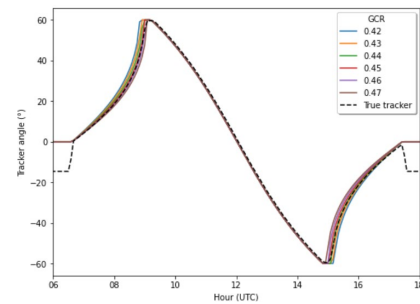


Fig. 3 Comparison between measured tilt angle of string 2 (black dotted curve) and modelled tilt angles. GCR: ground coverage ratio.

### 3.2. Front and back side irradiance

With the “pvfactors\_timeseries” function from PVlib, the front and back irradiance received by the test module were computed using the previously obtained tilt angles, and on-site measurements such as diffuse horizontal irradiance, direct normal irradiance, albedo, and installation geometry.

The relative mean bias error (rMBE) was calculated for both the period in horizontal position and in backtracking mode.

When in a horizontal position, for the front cell there is a rMBE of 3.64% and for the back cell of -5.28% while in backtracking mode the errors increase to 7.84% and -8.10%, respectively.

Having the front and back irradiances along with the known bifaciality factor, it is now possible to calculate the effective irradiance, which includes contributions from both front and back sides, using (1). Said effective irradiance will later be used to model the power output of the module.

$$G_{eff} = POA_{front} + (POA_{back} * \varphi_{Pmax}) \quad (1)$$

Hereafter, two effective irradiances will be referred to: modelled and measured effective irradiance. The modelled one was calculated using the modelled back and front irradiances while the measured one was calculated using on-site measurements from the reference cells located on the test module as shown in Fig. 2.

When comparing the two effective irradiances for both periods, there is an increase in rMBE from 2.74% when in horizontal position to 6.48% when in backtracking mode. If the difference in position is not considered, there is a good agreement between both with a rMBE of 4.04%. The low error is because the main contribution comes from the irradiance received on the front side of the module.

### 3.2.1 Albedo effect

Having had two full cycles of crop growth during the period of study, their influence on the albedo was explored. In Fig. 4, the daily albedo value calculated with measurements from the meteorological station is presented, along with the dates of crop growth and recollection. During the first cycle of crop growth there is an increase in albedo of 4%. Once the first crop cycle was recollected, a decrease in albedo of 2% was observed. Followed by a subsequent increase in albedo due to a second cycle of crop growth. Although a third cycle is not yet completed, an upward trend is visible.

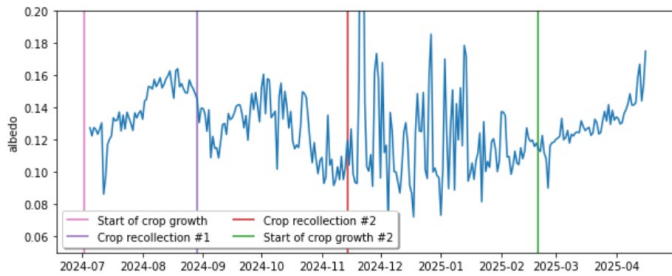


Figure 4 Daily values of albedo calculated with measurements from meteorological station. The colored lines indicate events such as crop growth and recollection.

During the period in horizontal position, the influence of crop presence on modelling errors is explored using 2 cloudy days as an example: June 6<sup>th</sup> and August 4<sup>th</sup>, their corresponding pictures are shown in Figure 5.



Figure 5 Picture of agrivoltaic installation with bare soil (left) and with presence of crop (right). They correspond to June 6<sup>th</sup> and August 4<sup>th</sup> 2024 respectively.

When comparing the measured and modelled values for back irradiance for these two days the change in rMBE is noticeable. When the soil is bare there is a rMBE of -6.02 % and with the presence of plants, it increases to -23.16 %. This shows both the adequacy of the model and the need to consider a changing albedo when there is the presence of growing plants.

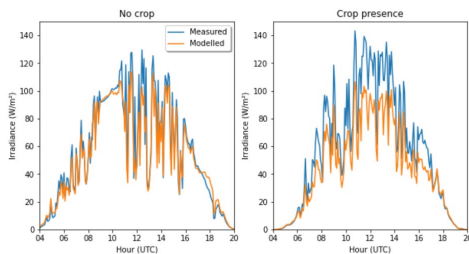


Figure 6 Comparison between measured (blue) and modelled (orange) back irradiance. The left frame corresponds to June 6<sup>th</sup> 2024 where there is no crop presence and the right one to August 4<sup>th</sup> 2024 where there is a significant growth of crop.

This sensitivity to an increase in albedo does not translate to the modelled values of the front irradiance as is shown in Fig. 7 since its rMBE changes only from 2.53% to 2.77%

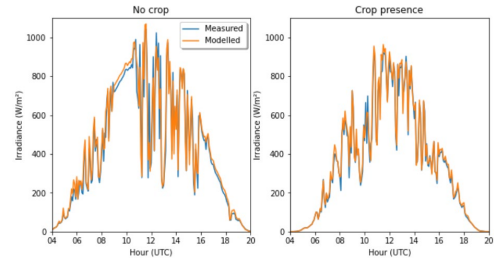


Figure 7 Comparison between measured (blue) and modelled (orange) front irradiance. The left frame corresponds to June 6<sup>th</sup> 2024 where there is no crop presence and the right one to August 4<sup>th</sup> 2024 where there is a significant growth of crop.

### 3.3. Module temperature

For the module temperature, three models were considered, the Faïman model [8], the SANDIA model [9], and the one provided in the PVsyst [10] commercial software.

Errors calculated for the period in horizontal position and backtracking mode are summarized in Table 1.

Table 1 Summary of error metrics between measured and modelled module temperature considering three different models, indicated with light orange. The cells with a white background correspond to a horizontal position and those in gray correspond to backtracking mode.

	MBE (°C)	MAE (°C)
Faïman	0.94	1.84
	0.60	1.33
SANDIA	1.73	2.15
	0.99	1.53
PVsyst	2.38	2.69
	1.30	1.76

These results indicate the Faïman model gives the best fit regardless of the module position. Further analyses indicate this remains true when looking at different types of day (sunny, variable, cloudy) with a maximum MBE of 1.46 °C for sunny days.

There was however a non-negligible overestimation at nighttime and midday after the crops were planted, suggesting the evapotranspiration from the crops may lower the temperature of the module.

### 3.4. DC Power

Finally, the power output of the module was estimated using the PVWatts model [11] due to its simplicity, utilizing the previously modelled and measured effective irradiance, and the module temperature. A power temperature coefficient of 0.30 %/°C was used, was provided by the manufacturer for the front face of the module.

In Table 2, a summary of the results for both horizontal and backtracking periods is presented. For each period a modelled and measured effective irradiance was used to model the power output.

Table 2 Summary of error metrics between measured and modelled power output using measured and modelled effective irradiance for horizontal and backtracking period. Light purple corresponds to using a measured effective irradiance and light green to a modelled one.

	MBE (W/m²)	rMBE (%)	MAE (W/m²)	rMAE (%)
Horizontal	13.34	8.80	14.27	9.42
	17.98	11.82	18.31	12.04
Backtracking	14.14	10.96	14.90	11.55
	21.13	16.08	21.50	16.36

From the table it can be seen that using a modelled effective irradiance instead of a measured one when in a horizontal position will result in an increase in rMBE of 3.02% while for

backtracking the increase will be of 5.12%. This is proportional to the rMBE of modelled irradiances discussed in section 3.2.

#### 4. PERFORMANCE CHARACTERIZATION

For the performance characterization, indicators such as reference yield, module yield, and performance ratio were calculated and analyzed.

##### 4.1. Reference Yield

The purpose of calculating the reference yield of the back reference cell was to explore whether the change of albedo discussed in section 3.2.1 would be observable. Shown in Fig. 10 is the monthly reference yield of both the front and back reference cells.

As expected, the highest reference yield of the front cell comes during summer, between June and August. It remains stable with maximum and minimum values of 804 and 783 hours, respectively.

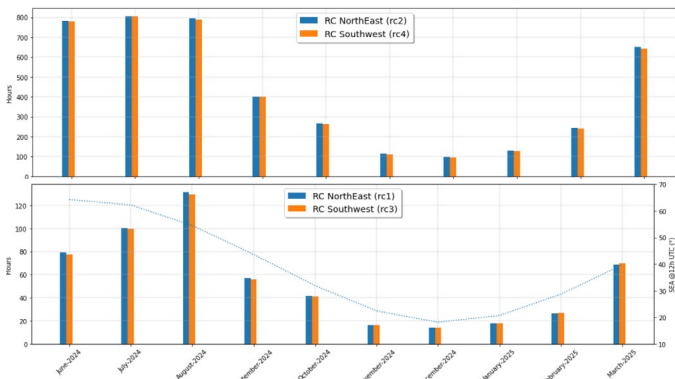


Figure 8 Monthly reference yield for front (first row) and back (second row) reference cells. The mean sun elevation angle (SEA) at noon is marked with a dotted blue line.

However, when looking at the reference yield of the back reference cell, an increase is noticeable between June and August. Since it coincides with the growth of alfalfa as shown in Fig. 5, the increase of albedo is believed to have contributed.

##### 4.2. Module Yield

When analyzing the module yield, the impact of shading on modules B1 and D1 by the meteorological station became evident.

Fig. 12 shows the yield of every module in groups A and B normalized by the yield of modules A1 and B1 respectively. A first observation is how for group A, the module yield slightly decreases towards the center with a maximum difference of 5% with respect to the first one. This is because the extremes have no obstacles close to them that block the incoming irradiance whereas those in the center have obstacles on both sides. The same behavior is observed for modules of group C although not shown.

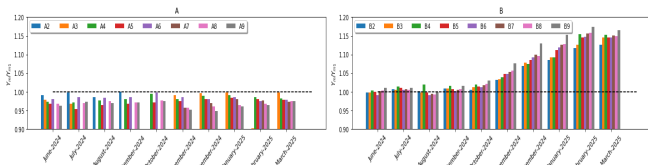


Figure 12 Monthly module yield of modules #2 - #9 of groups A and B normalized by the yield of modules A1 and B1 respectively.

Conversely, for group B the difference between module B1 (located in the center) and the one located on the edge would appear to increase with time. This is due to shading in the morning on module B1 caused by the central torque-tube that is part of the structure supporting the modules and in the afternoon by the sonic anemometer of the meteorological station. These shading effects are shown on Fig. 13. For module D1 shading is only present in the morning.

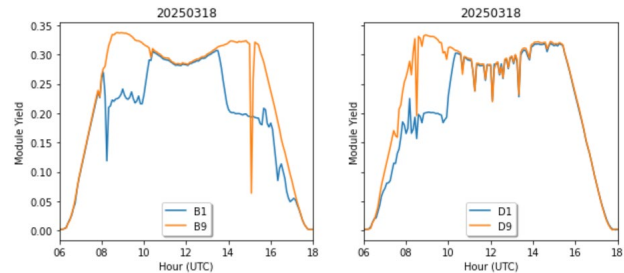


Figure 13 Module yield comparison of modules B1 and B9 (left) and D1 and D9 (right). The morning shade is caused by a torque-tube in the supporting structure while the one in the afternoon is caused by the sonic anemometer of the meteorological station.

##### 4.3. Performance Ratio

Analyzing the daily performance ratio (PR) of the test module provided insight on the impact soiling, change of albedo, and backtracking can have on the performance of the module.

Fig. 14 illustrates the daily PR variation of the module test as well as the precipitation at the installation in mm/day. The drop in PR of 6.63% between the 29<sup>th</sup> and 30<sup>th</sup> of June is due to soiling caused by a storm, as shown on Fig. 15. Following this event, the continuous increase in PR is attributed to the frequent rains keeping the module clean and the previously discussed increase in albedo since more irradiance is absorbed in the back face.

Overall, the consistent PR between 100 and 110 when in horizontal position highlights the advantage of utilizing bifacial modules. Furthermore, the change from a horizontal position to backtracking resulted in an increase in PR of 10.46%.

The impact of an increase in albedo is also noticeable in the PR change from 92.93% at the beginning of the first crop cycle to 103.41% when it was recollected.

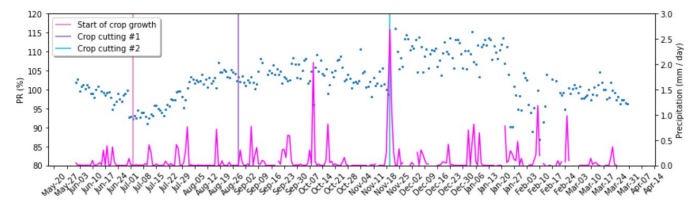


Figure 14 Daily performance ratio of test module. Daily precipitation in mm/day is marked by pink curved.



Figure 15 Aerial photo of clean modules on June 29<sup>th</sup> before storm (left) and June 30<sup>th</sup> where soiling is visible.

## 5. CONCLUSIONS

These preliminary results show the adequacy of existing irradiance, temperature, and power models to estimate the operation of a module in an agrivoltaic installation but also their limitations. While there is good agreement between measured and modelled values when in a horizontal position, the error increases once the module is in backtracking mode. It comes from the difficulty of accurately modelling the amount of irradiance received by the module as it moves throughout the day. This highlights the difficulty of modelling the power output of a non-fixed module.

The presence of crops underneath a PV module leads to an increase in the rear irradiance received by the backface of the module which contributes to a higher modelling error.

Furthermore, the study of individual module yield showed the impact shading can have on the production of a bifacial module. The layout of an installation can lead to modules located on the edge of the strings to give a higher yield than those located on the center due to a lack of obstacles blocking arriving irradiance.

Additionally, the effect of soiling on energy production is non-negligible, especially when in a horizontal position as deposited particulates will remain in place until a significant rain event removes them.

Finally, the analysis of the individual performance ratio of modules highlights the advantage of installing bifacial modules over monofacial ones, particularly during summer.

## 6. ACKNOWLEDGEMENTS

This work is part of the AgriPV-ER project (22-PETA-0007), which contributes to the “Pole National de Recherche on l’Agrivoltaïsme” from INRAE. The project is supported by France 2030, the PEPR TASE (<https://www.pepr-tase.fr/>), as well as the 3rd Programme d’Investissements d’Avenir [ANR-18-EUR-006-02], and the Foundation of Ecole polytechnique (Chaire “Défis Technologiques pour une Energie Responsable”) financed by TotalEnergies.

## 7. REFERENCES

- [1] P. Drobinski *et al.*, “Chapter 3 Resources | Subchapter 3.3 Energy transition in the Mediterranean”.
- [2] E. H. Adeh, S. P. Good, M. Calaf, and C. W. Higgins, “Solar PV Power Potential is Greatest Over Croplands,” *Sci. Rep.*, vol. 9, no. 1, p. 11442, Aug. 2019, doi: 10.1038/s41598-019-47803-3.
- [3] D. S. Charline, “Agrivoltaic system: a possible synergy between agriculture and solar energy”.
- [4] “Agrivoltaics Market Size to Surpass USD 13.88 Billion by 2034.” Accessed: May 19, 2025. [Online]. Available: <https://www.precedenceresearch.com/agrivoltaics-market>
- [5] X. Sun, M. R. Khan, C. Deline, and M. A. Alam, “Optimization and performance of bifacial solar modules: A global perspective,” *Appl. Energy*, vol. 212, pp. 1601–1610, Feb. 2018, doi: 10.1016/j.apenergy.2017.12.041.
- [6] S. Zainali, S. M. Lu, E. Potenza, B. Stridh, A. Avelin, and P. E. Campana, “3D View Factor Power Output Modelling of Bifacial Fixed, Single, and Dual-Axis Agrivoltaic Systems,” *Agrivoltaics Conf. Proc.*, vol. 2, May 2024, doi: 10.52825/agripv.v2i.1003.
- [7] M. Haeffelin *et al.*, “SIRTA, a ground-based atmospheric observatory for cloud and aerosol research,” *Ann. Geophys.*, vol. 23, no. 2, pp. 253–275, Feb. 2005, doi: 10.5194/angeo-23-253-2005.
- [8] D. Faiman, “Assessing the outdoor operating temperature of photovoltaic modules,” *Prog. Photovolt. Res. Appl.*, vol. 16, no. 4, pp. 307–315, Jun. 2008, doi: 10.1002/ppp.813.
- [9] J. Kratochvil, W. Boyson, and D. King, “Photovoltaic array performance model,” SAND2004-3535, 919131, Aug. 2004, doi: 10.2172/919131.
- [10] A. Mermoud, “PVSYST: A user-friendly software for PV-systems simulation”.
- [11] B. Marion, “Comparison of predictive models for photovoltaic module performance,” in *2008 33rd IEEE Photovoltaic Specialists Conference*, San Diego, CA, USA: IEEE, May 2008, pp. 1–6. doi: 10.1109/PVSC.2008.4922586.